

Amplification of near-infrared light in a photorefractive ring resonator

Malgosia Kaczmarek*, Roger S. Cudney*, Robert W. Eason #

*Department of Physics and Astronomy and Optoelectronics Research Centre #, University of
Southampton, Southampton SO17 1BJ, United Kingdom

Tel: +44 23 8059 2098

Fax: +44 23 8059 3142

e-mail: M.Kaczmarek@exeter.ac.uk

* División de Física Aplicada, CICESE, Apdo. Postal 2732, Ensenada, B.C, C.P. 22880, Mexico

Abstract

We have demonstrated efficient amplification of near-infrared, 0.83 μm and 1.06 μm light, in a photorefractive ring resonator using Rh:BaTiO₃. The optical power oscillating inside the ring exceeded the pump power by up to a factor of 2.34. The sensitivity of a ring resonator to nanometer changes in its length was characterised using a piezo mirror.

PACS numbers: 42.65.Hw, 42.70.Nq, 42.60.Da

Submitted to Applied Physics B
(Nov 2000)

1. Background

Photorefractive resonators have been the subject of several investigations over the past few years. In particular, theoretical analysis of their spatiotemporal [1] and nonlinear dynamics [2], stability [3], transverse [4] and coherence [5] effects have been extensively researched.

One of the resonator's geometries – unidirectional ring resonator – has proved particularly interesting because of its unique features. Its geometry is often very tolerant to misalignment, as the gratings that develop are self-adaptive and will grow from small seed beams, such as scattered light, if the process is favourable. The resonating beam accumulates energy from successive two-beam coupling amplification on each round trip through the photorefractive material until saturation sets in, but loses energy from absorption and other losses such as Fresnel reflections from the crystal, and imperfect mirrors. The resonating beam builds up providing the coupling efficiency exceeds the combined absorption and resonator losses. Such a ring resonator has the capability of providing large amplification of weak signals and being very sensitive to minute changes in its length.

The first successful demonstrations of unidirectional ring resonators were carried out by White *et al.* [6], Kwong *et al.* [7] and Ewbank *et al.* [8] in which it was discovered that small frequency detuning effects exist between the pump beam and the oscillation beam in photorefractive oscillators. They investigated threshold conditions for oscillations and the maximum permissible cavity-length detuning. A ring resonator can support oscillations over a wide range of cavity detuning in spite of a narrow, typically few Hz, photorefractive gain. As has been shown, this is due to photorefractive phase shift which can compensate for cavity detuning and thus help to fulfil the round-trip resonator condition [9].

In characterising the performance of a photorefractive ring resonator, it is useful to consider two parameters. One of them – the conversion efficiency ξ – is the power conversion from the

external pump beam into the resonating beam inside the cavity, defined as a ratio of the resonating beam power P_{out} to the power of the external pump beam P_{int} , which is given by [10]

$$\xi = \frac{P_{res}}{P_{pump}} = \frac{R_{out} - e^{(\alpha_{eff} - \Gamma)L}}{e^{\alpha_{eff}L} - R_{out}} \quad (1)$$

where R_{out} is the out-coupling mirror reflectivity, Γ is the two-beam coupling coefficient, L is the length of the interaction region inside the photorefractive material, and α_{eff} is the effective absorption coefficient that includes combined losses from the crystal, absorption, mirror and Fresnel reflection losses. This equation is valid above threshold of oscillations.

The other parameter that characterises photorefractive ring-resonators is the efficiency of extracting energy from the resonator. It is defined as the ratio of the power of light out-coupled from the resonator (P_{out}) to the power of the external pump beam (P_{pump}) [10]:

$$\eta = \frac{P_{out}}{P_{pump}} = \frac{1 - R_{out}}{R_{out}} \frac{R_{out} - e^{(\alpha_{eff} - \Gamma)L}}{e^{\alpha_{eff}L} - R_{out}} \quad (2)$$

As can be seen from equation (1), the conversion factor ξ can be larger than 1 if the coupling coefficient significantly exceeds absorption and reflection losses. However, in all previously published papers on photorefractive ring resonators, they have been pumped by visible light, i.e. in the regimes where absorption was high and therefore no net amplification was observed. In the work presented here, we have successfully demonstrated the build-up and amplification of power in a ring resonator using a near to optimum wavelength, using material and optical component parameters established earlier [11]. We report on efficiently working resonators pumped by near infrared, 830 nm and 1.06 μm lasers. The power oscillating in the 1.06 μm resonator exceeded the power of the pump beam.

2. Experimental configuration

The experimental configuration consisted of three mirrors and a photorefractive crystal, which was a sample of infrared sensitive Rh:BaTiO₃, pumped by cw near-infrared, single longitudinal mode lasers. In the first case this was a 300 mW diode-pumped Nd:YAG laser emitting light at 1064 nm and in the second experiment a 100 mW, 830 nm diode laser. Both lasers formed spot sizes of 3 mm diameter on the input face of the crystal.

In the experiment, the pump beam incident on the crystal fans towards the +c face and some of the fanned light is directed around the loop to re-enter the crystal, via the three mirror set-up. The light in this ring is unidirectional because the two-beam coupling gain is itself directional as determined by the crystal's symmetry, alignment and the charge transport properties, so any backward travelling light will experience loss. If the two-beam coupling gain is above threshold, the resonating beam will build up from the progressive amplification of this fanned light. The circulating power can be easily determined by monitoring the power of the light transmitted by the output coupler of the cavity ($R < 100\%$). In the 1.06 μm resonator, the output coupler had 95% reflectivity, while in the 830 nm resonator, 4% of the resonating power was out-coupled. The power of light resonating inside the cavity was calculated from the measurement of out-coupled energy and the reflectivity of the coupler. In order to minimise the losses of the resonator, the remaining mirrors were 99.9% reflective.

With either the miniature Nd:YAG laser or a diode laser, the experimental set-up could be made quite compact. The length of the 830 nm resonator was 62 cm while the 1.06 μm resonator was 52 cm long. For the tests of the cavity sensitivity to the changes of path length, one of the high reflecting ($R=99.9\%$) mirrors was mounted on a piezoelectric actuator.

In our earlier theoretical studies^[11] we established that the most crucial parameters for an effective operation of a resonator are the wavelength of the pump light and the type of

photorefractive material. It is vital to keep the value of *absorption* to a minimum, while ideally also maximising the magnitude of coupling coefficient (by cutting or otherwise orienting the crystal, for example). Since the coupling coefficient and the absorption of a photorefractive material are strongly wavelength dependant, the most efficient operation is achieved through a careful selection of the wavelength of the external pump beam. For example, these low-loss conditions can be fulfilled in samples lightly doped with rhodium and in the near-infrared regime, where absorption is low (approximately $0.1\text{-}0.2\text{ cm}^{-1}$) yet coupling coefficients can be relatively high ($7\text{-}11\text{ cm}^{-1}$).

Following the characterisation of the crystals' absorption and two-beam coupling coefficients, we selected five samples to test the performance of the resonators at 830 nm and 1064 nm. The parameters of the crystals and resonators are given in table I and II.

3. Results and discussion

In the first stage of our experimental studies, we investigated the performance of the resonator at 830 nm, where inexpensive and miniature diode lasers exist, which are ideal as pumping sources. In this regime, absorption coefficients are relatively high for producing efficient resonating results ($\alpha_{\text{eff}} > 0.1\text{ cm}^{-1}$); however such a value of absorption means increased speed of the two-beam coupling process as compared with the $1.06\text{ }\mu\text{m}$ regime. Therefore a resonating beam builds-up faster than at $1.06\text{ }\mu\text{m}$ and the task of optimising the alignment of the cavity is made easier. Figure 1 presents a typical example of build-up of power in a 830 nm resonator with a crystal with relatively low absorption ($\alpha_0=0.4\text{ cm}^{-1}$). The variation in time of the amplified oscillating beam power are typical for a two-beam coupling interaction.

We demonstrated a ring resonator working with a 830 nm pump and in different samples of Rh:BaTiO₃. Its conversion efficiency was, as expected, below 100% ($\xi < 1$). Nevertheless, up to

87% of the incident pump power was converted into an oscillation beam that built-up to approximately an order of magnitude faster than in the case of a 1.06 μm pump beam. The comparison of the results measured at 830 nm are summarised in Table I.

In the following stage of our experimental work we achieved ring resonators working efficiently with several samples of Rh:BaTiO₃ at 1.06 μm wavelength. We have measured a build-up of power inside the resonator exceeding the pump beam by up to a factor of 2.34. The maximum power resonating inside the cavity was 586 mW for an incident pump of 250 mW. Figure 2 presents this case, where the oscillating power was monitored for approximately 300 seconds.

Table II provides the details of results obtained in samples tested inside the 1.06 μm resonator and their comparison with the theoretically predicted values of resonating power. As can be seen, there is a good agreement between experiment and theory. The difference for some samples, such as 3200 ppm crystal for example, can be related to effects such as strong laser induced absorption that would contribute to an increased effective absorption coefficient.

In principle, higher efficiency would be possible, as predicted by theory, if losses could be reduced. In our case, the optimum two-beam coupling geometry required incidence angles where Fresnel losses were considerable. While the input pump beam's incidence angle was close to the Brewster angle (69°), the angle of incidence of the resonating beam (29°) meant that high Fresnel losses, of the order of 23%, accumulated. Swapping the beams and rotating the crystal to make the resonating beam incident at Brewster's angle reduced the losses, but yielded a much lower value of coupling coefficient. Therefore, in order to achieve higher oscillating power, anti-reflection coating of the crystal or selecting the optimum crystal cut would have to be carried out.

The parameters of a photorefractive crystal, cavity losses and pumping light are not the only critical factors that have to be taken into account to ensure the efficient oscillations. In aligning the resonators we also noted the importance of correct cavity alignment via its mirrors. Although photorefractive ring resonators can adapt their operation to different cavity lengths, they are very sensitive to imperfections and tilts in cavity alignment. Minute cavity distortions can prevent the build up of oscillations or if the degree of misalignment is small, cause additional, high-order modes to appear [12].

Finally, we determined the stability and sensitivity to cavity path length changes on the resonating beam. Using a piezo-mirror as one of the cavity mirrors, we established that sub-nanometer changes could be detected. The high sensitivity to cavity mismatch in the high gain ring cavity pumped by a 1064 nm beam was also confirmed. Figure 3 shows the variation in the oscillation beam intensity with time as the piezo mirror is moved by up to 1.5 nm.

Such high sensitivity to nanometer changes in cavity length is ideally suited for sensing applications where, for example, minute concentrations of trace species could be measured. However, although satisfactory long term stability (figure 2) could be achieved, the power fluctuations we observed would mask out any sensitive refractive index changes measured. An active stabilisation of the cavity, namely a piezo-mirror with a feedback device [13] should resolve this difficulty. We plan to explore this improvement of the cavity design to achieve higher amplification ratios.

4. Conclusions

This is the first report, to our knowledge, of a photorefractive ring resonator working at wavelengths at 830 nm and above 1 μm . In this regime, due to low absorption and sufficiently

high coupling coefficients, significant amplification of a diffraction-limited oscillation beam was observed, exceeding the input pump beam power by a factor up to 2.34. We also showed that such efficiently working photorefractive cavity is sensitive to sub-nanometer changes in cavity length.

5. Acknowledgements

We would like to thank Jack Feinberg for providing us with Rh:BaTiO₃ samples and for the useful advice and discussions on this work. We gratefully acknowledge the financial support of the Royal Society Research Grant Scheme, the Engineering and Physical Sciences Research Council under grant number GR/M/11844 and under their Advanced Fellowship scheme.

Figure captions

Table I Experimentally determined parameters of performance of ring resonators and Rh:BaTiO₃ crystals at 830 nm.

Γ : two beam coupling coefficient; α_o : small signal absorption coefficient; α_{eff} : effective absorption coefficient that includes reflection losses; $\xi_{exp} = P_{res}/P_{pump}$ – intensity conversion factor measured experimentally.

Table II Experimentally determined parameters of performance of ring resonators and Rh:BaTiO₃ crystals at 1.06 μm with 250 mW pump beam.

Γ : two beam coupling coefficient; α_o : small signal absorption coefficient; α_{eff} : effective absorption coefficient that includes reflection losses; P_{res} : intensity resonating inside the cavity; P_{out} : measured intensity, out-coupled from the resonator; $\xi_{exp} = P_{res}/P_{pump}$ – intensity conversion factor measured experimentally; ξ_{th} : conversion factor predicted by the theory.

Figure 1 Build-up time of oscillation beam with an 98 mW, 830 nm pump beam and a Rh:BaTiO₃ crystal (JackB crystal with $\alpha_{eff} = 1.12 \text{ cm}^{-1}$)

Figure 2 Power of the oscillating beam and its stability in a cavity with JackA Rh:BaTiO₃ sample pumped by 1.06 μm beam.

Figure 3 Resonating beam power variation with time as a function of a movement of a piezo mirror. The cavity included Dan sample of Rh:BaTiO₃ pumped by 1.06 μm . Thick solid line: resonating power signal, thin solid line: variation in cavity length.

References:

- ¹ G. D' Alessandro, Phys. Rev. **46**, 2791 (1992).
- ² B. J. Jost, B. E. A. Saleh, J. Opt. Soc. Am. B **11**, 1864 (1994).
- ³ Z. Jun, T. Weihan, Phys. Rev. A **54**, 5201 (1996).
- ⁴ J. Leonardy, M. Belić, F. Kaiser, J. Opt. Soc. Am. B **15**, 1714 (1998).
- ⁵ W. Królikowski, Opt. Comm. **129**, 44 (1996).
- ⁶ J. O. White, M. Cronin-Golomb, B. Fischer, A. Yariv, Appl. Phys. Lett. **40**, 450 (1992)
- ⁷ S. Kwong, A. Yariv, M. Cronin-Golomb, I. Ury, Appl. Phys. Lett. **47** 460 (1985).
- ⁸ M. D. Ewbank, P. Yeh, Opt. Lett. **10**, 496 (1985).
- ⁹ P. Yeh, J. Opt. Soc. Am. B, **2**, 1924, (1985).
- ¹⁰ P. Gunter and J.-P. Huignard (editors) *Photorefractive Materials and Their Applications vol. II'*, Topics in Applied Physics vol. 62, (Springer, Berlin, Heidelberg 1989).
- ¹¹ M. Kaczmarek, R. W. Eason, Opt. Comm. **154** 334 (1998).
- ¹² A. Mazur, S. Odoulov, IEEE J. Quant. Elec. **26**, 963 (1990).
- ¹³ G. Balzer, C. Denz, O. Knaup, T. Tschudi, Chaos solitons & fractals, **10**, 725 (1999)

Table I

Crystal	Γ [cm^{-1}]	α_o [cm^{-1}]	α_{eff} [cm^{-1}]	ξ_{exp}
Dan	10	1.2	1.76	0.38
JackA	12.3	0.15	0.8	0.84
400ppm	11.6	0.29	0.84	0.68
3200ppm	11	3.61	4.32	0.17
Jack B	10.6	0.4	1.12	0.87

Table II

Crystal	Γ [cm^{-1}]	α_o [cm^{-1}]	α_{eff} [cm^{-1}]	P_{res} [mW]	P_{out} [mW]	ξ_{exp}	ξ_{th}
Dan	10.1	0.05	0.59	560	28	2.24	2.398
JackA	10.4	0.07	0.69	586	29.5	2.344	2.34
400ppm	8.3	0.03	0.56	520	26	2.08	2.459
3200ppm	9	0.25	1.24	226	11.5	0.904	1.339

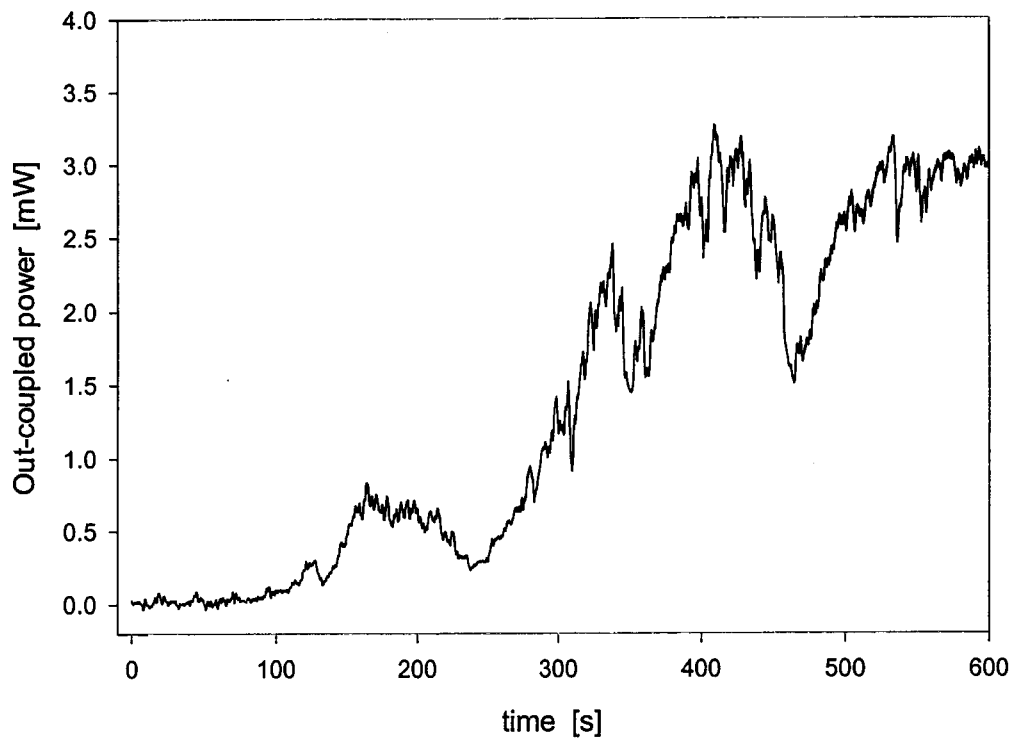


Fig 1

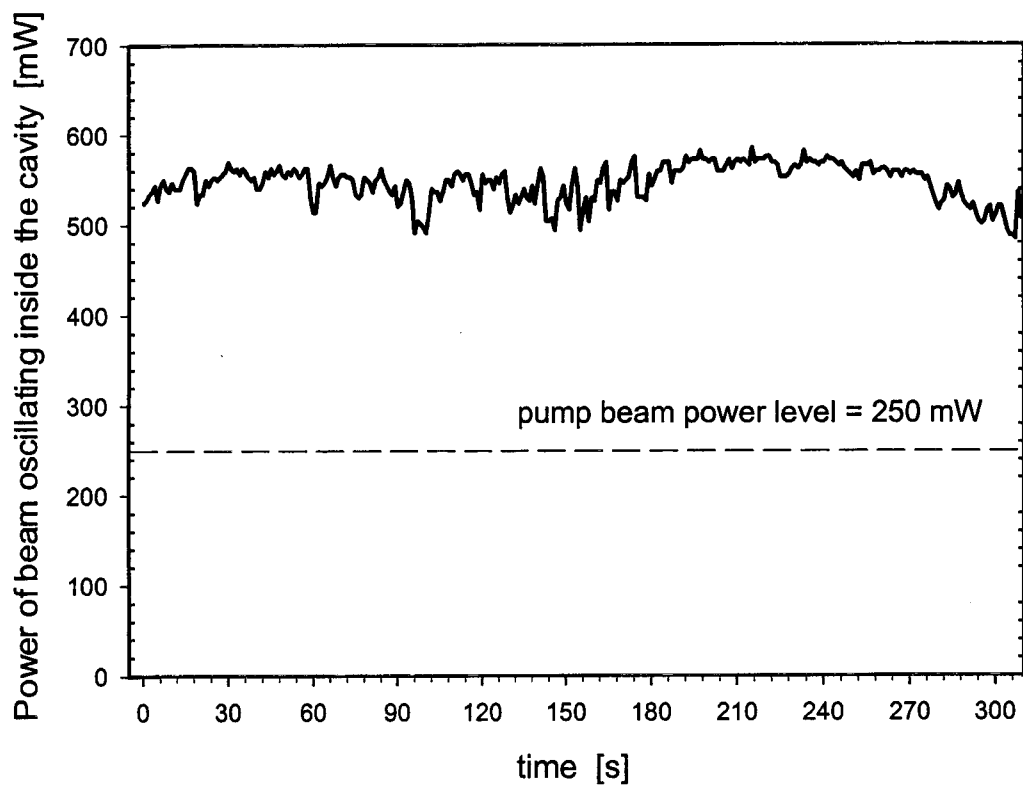


Fig 2

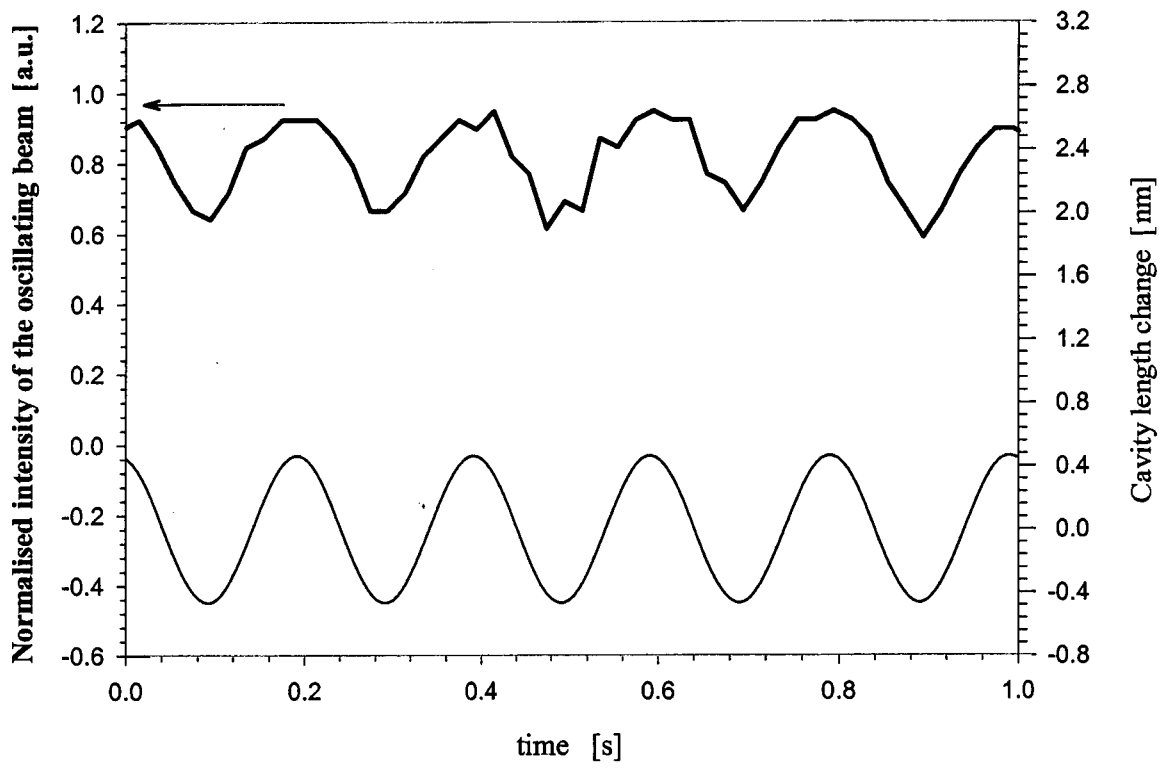


Fig 3